

## Herpes Simplex Virus 1 Protein Kinase Us3 Phosphorylates Viral Envelope Glycoprotein B and Regulates Its Expression on the Cell Surface<sup>∇</sup>

Akihisa Kato,<sup>1†</sup> Jun Ariei,<sup>1,2†</sup> Ikuo Shiratori,<sup>3‡</sup> Hiroomi Akashi,<sup>2</sup>  
Hisashi Arase,<sup>3,4</sup> and Yasushi Kawaguchi<sup>1\*</sup>

Division of Viral Infection, Department of Infectious Disease Control, International Research Center for Infectious Diseases, The Institute of Medical Science, The University of Tokyo, Minato-ku, Tokyo 108-8639,<sup>1</sup> Department of Veterinary Microbiology, Graduate School of Agricultural and Life Science, The University of Tokyo, Bunkyo-ku, Tokyo 113-8657,<sup>2</sup> Laboratory of Immunochemistry, Research Institute for Microbial Diseases and WPI Immunology Frontier Research Center, Osaka University, Suita, Osaka 565-0871<sup>3</sup>, and SORT, JST, Saitama 332-0012,<sup>4</sup> Japan

Received 11 July 2008/Accepted 15 October 2008

**Us3 is a serine-threonine protein kinase encoded by herpes simplex virus 1 (HSV-1). As reported here, we attempted to identify the previously unreported physiological substrate of Us3 in HSV-1-infected cells. Our results were as follows. (i) Bioinformatics analysis predicted two putative Us3 phosphorylation sites in the viral envelope glycoprotein B (gB) at codons 557 to 562 (RRVSAR) and codons 884 to 889 (RRNTNY). (ii) In in vitro kinase assays, the threonine residue at position 887 (Thr-887) in the gB domain was specifically phosphorylated by Us3, while the serine residue at position 560 was not. (iii) The phosphorylation of gB Thr-887 in Vero cells infected with wild-type HSV-1 was specifically detected using an antibody that recognized phosphorylated serine or threonine residues with arginine at the –3 and –2 positions. (iv) The phosphorylation of gB Thr-887 in infected cells was dependent on the kinase activity of Us3. (v) The replacement of Thr-887 with alanine markedly upregulated the cell surface expression of gB in infected cells, whereas replacement with aspartic acid, which sometimes mimics constitutive phosphorylation, restored the wild-type phenotype. The upregulation of gB expression on the cell surface also was observed in cells infected with a recombinant HSV-1 encoding catalytically inactive Us3. These results supported the hypothesis that Us3 phosphorylates gB and downregulates the cell surface expression of gB in HSV-1-infected cells.**

Phosphorylation is one of the most common and effective modifications by which a cell or virus regulates protein activity (9, 28). This modification is mediated by protein kinases that phosphorylate specific proteins, thereby regulating many cellular functions, such as transcription, translation, cell cycle regulation, protein degradation, protein intracellular trafficking, and apoptosis (9, 28). Herpes simplex virus 1 (HSV-1) encodes at least three protein kinases (the Us3, UL13, and UL39 gene products) and may utilize them both to regulate their own replication processes and to modify cellular processes by the phosphorylation of specific viral and cellular proteins (21, 46). This report presents studies of the interaction between Us3 protein kinase and HSV-1 envelope glycoprotein B (gB). The background for these studies is as follows.

(i) gB is conserved throughout the *Herpesviridae* family (39). It is an essential envelope glycoprotein for HSV-1 entry into a cell (54) and, together with HSV-1 glycoprotein gC, mediates virus attachment by interacting with cell surface glycosaminoglycans, primarily heparin sulfate (53). gB also induces subsequent fusion between the virion envelope, and the host cell

membrane, in cooperation with the HSV-1 glycoprotein heterodimer gH/gL, delivers the nucleocapsid into the host cell (54). Membrane fusion also requires HSV-1 gD binding to one of its receptors (e.g., herpesvirus entry mediator, nectin-1, and specific sites on heparin sulfate generated by certain 3-*O*-sulfotransferases [16, 31, 52, 59]) and, probably, gB binding to one of its receptors, including the newly discovered gB-associated cellular protein paired immunoglobulin (Ig)-like type 2 receptor (PILR $\alpha$ ) (2, 51). In addition to its role in virus entry, gB has been reported to function in cell-to-cell spread (14, 60) and the nuclear egress of nucleocapsids (13).

(ii) Us3 is a serine/threonine protein kinase, and its amino acid sequence is conserved in the subfamily *Alphaherpesvirinae* (15, 29, 41). In vitro biochemical studies characterized the consensus target sequence of an HSV-1 Us3 homologue encoded by pseudorabies virus as RnX(S/T)YY, where *n* is greater than or equal to 2, X can be Arg, Ala, Val, Pro, or Ser, and Y can be any amino acid except an acidic residue (25, 26, 40). The phosphorylation target site specificity of HSV-1 and other alphaherpesvirus Us3 kinases has been reported to be similar to that of the pseudorabies virus homologue and to that of protein kinase A (PKA), a cellular cyclic AMP-dependent protein kinase (3, 8, 10, 18). Antibodies to phosphorylated sequences of PKA substrates sometimes react with the site phosphorylated by Us3 (3, 18).

(iii) Based on studies showing that recombinant Us3 mutant viruses have impaired growth properties in cell cultures and virulence in mice models (30, 45), it has been concluded that HSV-1 Us3 is a positive regulator of viral replication and pathogenicity. Possible Us3 functions related to viral replica-

\* Corresponding author. Mailing address: Division of Viral Infection, Department of Infectious Disease Control, International Research Center for Infectious Diseases, The Institute of Medical Science, The University of Tokyo, 4-6-1 Shirokanedai, Minato-ku, Tokyo 108-8639, Japan. Phone: 81-3-6409-2070. Fax: 81-3-6409-2072. E-mail: ykawagu@ims.u-tokyo.ac.jp.

† A.K. and J.A. contributed equally to this work.

‡ Present address: Research Institute for Biological Sciences, Tokyo University of Science, 2669 Yamazaki, Noda, Chiba 278-0022, Japan.

<sup>∇</sup> Published ahead of print on 22 October 2008.

tion and pathogenicity have been gradually elucidated; e.g., to block apoptosis induced by both viral and cellular proteins (27, 34, 35, 37), to regulate the nuclear egress of progeny nucleocapsids (44, 45), and to control the morphology of infected cells (18, 36). Although the critical Us3 substrate(s) that mediates its functions has not yet been identified and, therefore, the molecular mechanisms by which Us3 acts remain largely unknown at present, these observations suggest that the Us3 protein kinase is a multifunctional enzyme that plays important roles in viral replication. This hypothesis predicts that there are many additional Us3 substrates different from those reported to date, and their identification and characterization are required to determine the function(s) of Us3 and to understand their mechanism(s).

In the present study, we identified gB as a physiological substrate of Us3 in HSV-1-infected cells. We also present evidence that the Us3 phosphorylation of gB downregulates the expression of the viral envelope glycoprotein on the cell surface in infected cells.

**MATERIALS AND METHODS**

**Cells and viruses.** Vero, rabbit skin, human embryonic lung fibroblast (HEL), SK-N-SH, and *Spodoptera frugiperda* Sf9 cells were described previously (18, 20, 22, 55), as was HSV-1 wild-type strain HSV-1(F) (12, 55). PILR ligand-negative CHO-K1 cells (51) were maintained in F12 medium supplemented with 10% fetal calf serum (FCS). Plat-GP cells, from a 293T-derived murine leukemia virus-based packaging cell line (32), were kindly provided by Toshio Kitamura and maintained in Dulbecco's modified Eagle's medium supplemented with 10% FCS. Recombinant virus YK511, encoding an enzymatically inactive Us3 mutant in which lysine at position 220 was replaced with methionine (Us3K220M); recombinant virus YK513, in which a K220M mutation in YK511 was repaired; and recombinant virus YK333, which expresses enhanced green fluorescent protein driven by the Egr-1 promoter, were described previously (18, 56). YK333 grew as well as wild-type HSV-1(F) in cell cultures, and only cells infected with YK333 expressed enhanced green fluorescent protein (56).

**Plasmids.** To generate a fusion protein of maltose binding protein (MBP) and part of gB, plasmids pMAL-gB-P1 and pMAL-gB-P2 were constructed by amplifying the domains encoding gB codons 448 to 628 and 772 to 904, respectively, by PCR from pCRxgB (51) and cloning the DNA fragments into pMAL-c (New England BioLabs) in frame with MBP. We note that the gB of HSV-1 F strain lacks an amino acid in the signal sequence that is found in HSV-1 KOS and 17 strains (38). To avoid confusion, we use the numbering of gB amino acids with the sequence of the KOS strain here. To generate a fusion protein of MBP fused to a mutated part of gB in which the threonine at gB position 887 (Thr-887) was replaced with an alanine (T887A), plasmid pMAL-gB-P2-T887A was constructed by amplifying the domain encoding gB codons 773 to 905 by PCR from pCRxgB using primers 5'-CGCAATTCCTCAACCCCTTTGGGGCGCTGGC-3' and 5'-GCGTCGACTCACAGGTCGTCCTCGTCGGCGCTCACCGTCTTTGTTGGGAAGCTTGGGTGTAGTTGGCGTTGCGGCGCTTGCATGAC-3', and cloning the DNA fragments into pMAL-c in frame with MBP. pMxs-mouse PILR (mPILR)-neo and pMxs-human nectin-1 (hnectin-1)-1-neo were constructed by cloning a cDNA fragment encoding mouse PILR $\alpha$  (58) and hnectin-1 (51), respectively, into pMxs-neo (kindly provided by Toshio Kitamura).

**Mutagenesis of viral genomes in *Escherichia coli* and generation of recombinant HSV-1.** To generate recombinant virus YK551, which carries an alanine replacement of Thr-887 in gB (gB-T887A) (Fig. 1), the two-step Red-mediated mutagenesis procedure was carried out using *E. coli* GS1783 containing pYEbac102 (55) (a kind gift from Gregory A. Smith and Nikolaus Osterrieder) as described previously (17, 18), except with primers 5'-CCAAGGTACCCGACA TGGTATCGCGCAAGCGCCGCAACGCCAACTACACCAAGTCCCAA GGATCAGCAGATAAGTAGGG-3' and 5'-GGCGTCACCGTCTTTGTTGG AACTTGGGTGTAGTTGGCGTTGCGGCGCTTGCATGACCAACC AATTAACCAATTCTGATTAG-3' (Fig. 1). pYEbac102 contained a complete HSV-1(F) sequence with the bacterial artificial chromosome (BAC) sequence inserted into the HSV intergenic region between UL3 and UL4 (55). Recombinant virus YK304, reconstituted from pYEbac102, has been shown to have a phenotype identical to that of wild-type HSV-1(F) in cell cultures and in a mouse

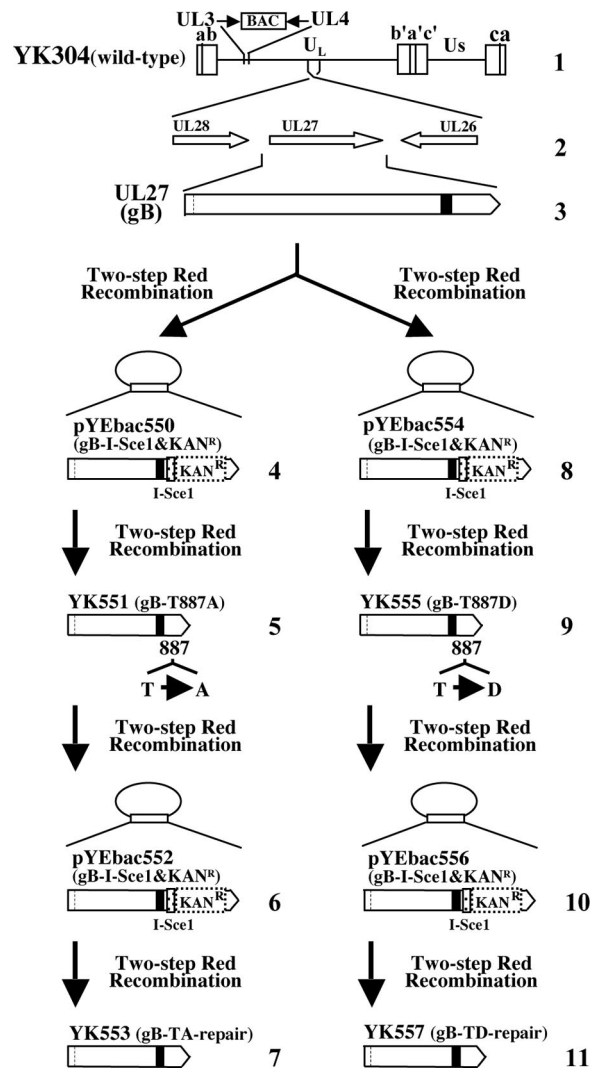


FIG. 1. Schematic diagram of the genome structures of wild-type YK304 and relevant domains of the recombinant viruses. Line 1, a linear representation of the YK304 genome. The unique sequences are represented as unique long (UL) and short (Us) domains, and the terminal repeats flanking them are shown as open rectangles with the designation above each repeat. The YK304 genome has bacmid (BAC) in the intergenic region between UL3 and UL4. Line 2, domains encoding the UL26, UL27 (gB), and UL28 open reading frames. Line 3, schema of the UL27 gene product (gB). The shaded area represents a trans-membrane domain. Lines 4, 6, 8, and 10 show schematic diagrams of plasmids pYEbac550, pYEbac552, pYEbac554, and pYEbac556, respectively. Lines 5 to 7, 9, and 11 show schematic diagrams of recombinant viruses YK551, YK553, YK555, and YK557, respectively.

model (55). As a result of the two-step Red-mediated mutagenesis procedure, *E. coli* strain GS1783(YEbac551) containing the mutant HSV-BAC plasmid pYEbac551, with the T887A mutation in gB (gB-T887A), was obtained. YK551 (Fig. 1) was generated by the transfection of pYEbac551 into rabbit skin cells as described previously (55). To generate recombinant virus YK553, in which the T887A mutation in YK551 gB was repaired (gB-TA-repair) (Fig. 1), the procedure to generate YK551 was used, except with *E. coli* YEbac551 and primers 5'-CCAAGGTACCCGACATGGTTCATGCGGCAAGCGCCGCAACCAAC TACACCAAGTTCACCAAGGATGACGACGATAAGTAGGG-3' and 5'-G GCGTCACCGTCTTTGTTGGGAAGCTTGGGTGTAGTTGGTGTGCGGC GCTTGCATGACCAACCAATTAACCAATTCTGATTAG-3'. Recombinant virus YK555, which carries an aspartic acid replacement of the Thr-887 in

gB (gB-T887D) (Fig. 1), was constructed by the procedure used to generate YK551, except with primers 5'-CCAAGGTCACCGACATGGTCATGCGCAA GCGCCGCAACGACAACACTACACCAAGTCCCAAGGATGACGACGAT AAGTAGGG-3' and 5'-GGCGTCACCGTCTTTGTTGGAACT TGGGTGTAGTTGTCGTTGCGGCGCTTGCGCATGACCAACCAATTA CCAATTCTGATTAG-3'. To generate recombinant virus YK557, in which the T887D mutation in YK555 gB was repaired (gB-TD-repair) (Fig. 1), the procedure to generate YK551 was used, except with *E. coli* YEbac555, which was obtained in the procedure to generate YK555 and contained pYEbac555 with a T887D mutation in gB, and primers 5'-CCAAGGTCACCGACATGGTCATG CCAAGCGCCGCAACACAACACTACACCAAGTCCCAAGGATGACG CGATAAGTAGGG-3' and 5'-GGCGTCACCGTCTTTGTTGGAACTTG GGTGTAGTTGTTGTCGCGCTTGCGCATGACCAACCAATTAAC AATTCTGATTAG-3'.

**Production and purification of MBP fusion proteins in *E. coli*.** MBP fusion proteins MBP-gB-P1, MBP-gB-P2, and MBP-gB-P2-T887A were expressed in *E. coli* that had been transformed with pMAL-gB-P1, pMAL-gB-P2, and pMAL-gB-P2-T887A, respectively, and purified as described previously (19).

**Antibodies.** Rabbit polyclonal antibody to Us3 was described previously (18). Phospho-PKA substrate (100G7) rabbit monoclonal antibody was purchased from Cell Signaling Technology. Mouse monoclonal antibodies to ICP0 (1112), gB (1105), and ICP4 (H640) were purchased from the Goodwin Institute. Mouse monoclonal antibody to gD (DL6), nectin-1 (CK8), and HSV VP5 (3B6) were purchased from Santa Cruz Biotechnology, Zymed Laboratories, and Virusys, respectively.

**Preparation of monoclonal antibody.** Rat monoclonal antibody to mouse PILR $\alpha$  (153) was generated as described previously (51), except that rats were immunized with mouse PILR $\alpha$ -Ig fusion protein.

**In vitro kinase assays.** MBP fusion proteins were captured on amylose beads (New England BioLabs) and used as substrates for in vitro kinase assays with 0.34  $\mu$ g (3.7 pmol) purified glutathione *S*-transferase (GST)-Us3 and GST-Us3K220M, as described previously (19). MBP fusion proteins were used as substrates for in vitro kinase assays, as described previously, with 0.45  $\mu$ g (11.9 pmol) purified PKA, which was purchased from Invitrogen (18).

**Immunoblotting and immunofluorescence.** Immunoblotting and indirect immunofluorescence assays were performed as described previously (24).

**Immunoprecipitation.** Immunoprecipitation was performed as described previously (18, 23), except HSV-1(F), YK511, YK513, YK551, YK553, and anti-gB antibodies were used.

**Phosphatase treatment.** MBP fusion proteins after in vitro kinase assays and immunoprecipitates were treated with phosphatase as described previously (19).

**Chemical treatments.** PKA inhibitor 6-22 amide was purchased from Calbiochem and used at a final concentration of 52 nM as described previously (23).

**Purification of virions.** Virions were purified as described previously (57).

**Generation of recombinant retroviruses and establishment of cell lines stably expressing mPILR $\alpha$  and hnectin-1.** Plat-GP cells (kindly provided by Toshio Kitamura) in a 24-well microplate were transfected by Lipofectamine (Invitrogen) with 0.5  $\mu$ g pMxs-neo, pMxs-mPILR-neo, or pMxs-hnectin-1-neo and 0.5  $\mu$ g pMDG (62), which expressed vesicular stomatitis virus envelope gG (kindly provided by Didier Trono). At 48 h posttransfection, culture supernatants were harvested. PILR ligand-negative CHO-K1 cells were transduced by infection with retrovirus-containing supernatants of transfected Plat-GP cells and selected with 0.5 mg G418 (Nacalai Tesque) per ml in maintenance medium. Resistant cells transduced by pMxs-neo-derived retrovirus were designated CHO-neo cells. Single colonies transduced by pMxs-mPILR-neo- and pMxs-hnectin-1-neo-derived retrovirus were isolated after 1 to 2 weeks and screened by infection with YK333, which led to the identification of CHO-mPILR $\alpha$  and CHO-hnectin-1 cells, respectively. The expression of hnectin-1 and mPILR $\alpha$  was confirmed by flow cytometry with antibodies to nectin-1 and PILR $\alpha$  (data not shown).

**Flow cytometry.** To analyze the cell surface expression of viral glycoproteins, infected adherent Vero or HEL cells were detached in phosphate-buffered saline (PBS) containing 0.02% EDTA and washed once with PBS supplemented with 2% FCS (washing buffer). To analyze the total expression of gB, infected Vero cells were detached as described above, fixed in 4% paraformaldehyde in PBS, and then permeabilized with 0.1% Triton X-100 in PBS. Cells with or without fixation were incubated with mouse monoclonal antibodies to gB or gD in wash buffer on ice for 30 min. After the cells were washed with washing buffer, they were further incubated with anti-mouse IgG conjugated to Alexa Fluor 488 (Invitrogen). After the cells were washed again, they were analyzed with a FACSCalibur with Cell Quest software (Becton Dickinson).

## RESULTS

### Identification of the Us3 phosphorylation site of gB in vitro.

We previously identified a physiological autophosphorylation site of Us3 by a combination of bioinformatics prediction, in vitro kinase assays for Us3, and the detection of phosphorylation in infected cells with anti-phospho-PKA substrate antibody 100G7, which detects proteins containing a phosphorylated serine or threonine residue with an arginine at positions -3 and -2 (RRXS or RRXT) (18). In the present study, we applied this system to identify the previously unreported Us3 substrate and its phosphorylation site(s). Based on the Us3 phosphorylation site consensus sequence, we identified two putative Us3 phosphorylation sites in gB, at codons 557 to 562 (RRVSAR) and codons 884 to 889 (RRNTNY) (Fig. 2A). To confirm that gB Ser-560 and/or Thr-887 are in fact the Us3 phosphorylation sites in vitro, we generated and purified chimeric proteins consisting of MBP fused to peptides encoded by gB codons 448 to 628 (MBP-gB-P1) and codons 772 to 904 (MBP-gB-P2) (Fig. 2A). The MBP fusion proteins were captured on amylose beads and used as substrates for in vitro kinase assays with purified wild-type GST-Us3 and the kinase-negative mutant GST-Us3K220M. As shown in Fig. 2C, MBP-gB-P2 was labeled with [ $\gamma$ -<sup>32</sup>P]ATP in kinase assays using GST-Us3 (Fig. 2C, lane 3), while MBP-gB-P1 was not (Fig. 2C, lane 1). When the kinase-negative mutant GST-Us3K220M was used, none of the MBP fusion proteins were labeled (Fig. 2C, lanes 2 and 4). To confirm that MBP-gB-P2 labeling by GST-Us3 was due to phosphorylation, the labeled MBP-gB-P2 was treated with  $\lambda$ -phosphatase ( $\lambda$ -PPase). As shown in Fig. 2E, MBP-gB-P2 labeling by GST-Us3 was eliminated by phosphatase treatment, indicating that MBP-gB-P2 was labeled by phosphorylation. The presence of each MBP fusion protein and the radiolabeled MBP-gB-P2 band were verified by Coomassie brilliant blue (CBB) staining (Fig. 2B and D). These results indicated that Us3 specifically and directly phosphorylated the gB peptide encoded by codons 772 to 904 in vitro.

We then generated and purified a mutated version of MBP-gB-P2 (MBP-gB-P2-T887A) in which alanine was substituted for Thr-887 (Fig. 2A) and tested it with in vitro kinase assays to examine if gB Thr-887 was the Us3 phosphorylation site in vitro. As shown in Fig. 2G, MBP-gB-P2 was labeled with [ $\gamma$ -<sup>32</sup>P]ATP in kinase assays using GST-Us3 (Fig. 2G, lane 1), while MBP-gB-P2-T887A was not (Fig. 2G, lane 3). When the kinase-negative mutant GST-Us3K220M was used, none of the MBP fusion proteins were labeled (Fig. 2G, lanes 2 and 4). The presence of each MBP fusion protein and the radiolabeled MBP-gB-P2 band was verified by CBB staining (Fig. 2F). These results indicated that gB Thr-887 was the in vitro Us3 phosphorylation site.

**PKA phosphorylation of gB Thr-887 in vitro.** An earlier report has shown that Us3 and PKA phosphorylate the same target protein site in vitro (3, 18). This observation led us to test whether PKA also phosphorylates gB Thr-887 in vitro. As shown in Fig. 3B, MBP-gB-P2 was labeled with [ $\gamma$ -<sup>32</sup>P]ATP in kinase assays using purified PKA (Fig. 3B, lane 2), while MBP-gB-P1 was not (Fig. 3B, lane 1). MBP-gB-P2 labeling by PKA was eliminated by phosphatase treatment (Fig. 3D), indicating that MBP-gB-P2 was labeled by phosphorylation. This phosphorylation was due to PKA based on the observation that



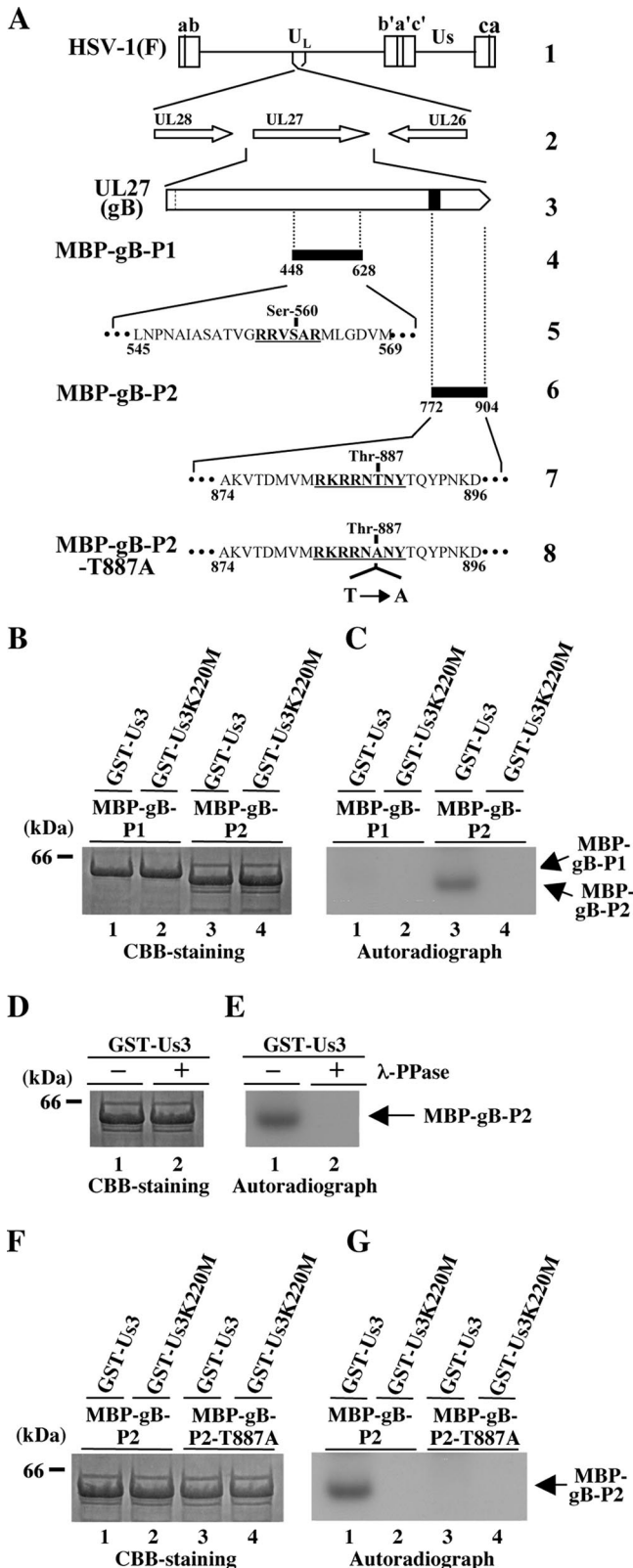


FIG. 2. (A) Schematic diagram of the genome of wild-type HSV-1(F) and the location of the UL27 (gB) gene. Line 1, linear representation of the HSV-1(F) genome. Line 2, the structure of the genome domain containing the UL26, UL27, and UL28 open reading frames. Line 3, the structure of the UL27 (gB) open reading frame. The

shaded area represents a *trans*-membrane domain. Line 4, the domain of the UL27 (gB) gene encoding gB residues 448 to 628, which were used in these studies to generate the MBP-gB-P1 fusion protein. Line 5, the amino acid sequence of gB residues 545 to 569. Sites with the consensus sequence for phosphorylation by Us3 are underlined. Line 6, the domain of the UL27 (gB) gene encoding gB residues 772 to 904, which were used in these studies to generate the MBP-gB-P2 fusion protein. Line 7, the amino acid sequence of gB residues 874 to 896. Sites with the consensus sequence for phosphorylation by Us3 are underlined. Line 8, the domain of the Us3 gene encoding gB residues 772 to 904 with the T887A mutation used in these studies to generate the MBP-gB-P2-T887A fusion protein. (B) Purified MBP-gB-P1 (lanes 1 and 2) and MBP-gB-P2 (lanes 3 and 4) incubated in kinase buffer containing [ $\gamma$ -<sup>32</sup>P]ATP and purified GST-U<sub>s3</sub> (lanes 1 and 3) or GST-U<sub>s3</sub>K220M (lanes 2 and 4), separated on a denaturing gel, and stained with CBB. A molecular mass marker (in kilodaltons) is shown on the left. (C) Autoradiograph of the gel in panel B. (D) Purified MBP-gB-P2 incubated in kinase buffer containing [ $\gamma$ -<sup>32</sup>P]ATP and purified GST-U<sub>s3</sub> and then either mock treated (lane 1) or treated with  $\lambda$ -PPase (lane 2), separated on a denaturing gel, and stained with CBB. A molecular mass marker (in kilodaltons) is shown on the left. (E) Autoradiograph of the gel in panel D. (F) Purified MBP-gB-P2 (lanes 1 and 2) and MBP-gB-P2-T887A (lanes 3 and 4) incubated in kinase buffer containing [ $\gamma$ -<sup>32</sup>P]ATP and purified GST-U<sub>s3</sub> (lanes 1 and 3) or GST-U<sub>s3</sub>K220M (lanes 2 and 4), separated on a denaturing gel, and stained with CBB. A molecular mass marker (in kilodaltons) is shown on the left. (G) Autoradiograph of the gel in panel F.

MBP-gB-P2 was not phosphorylated in the presence of a specific inhibitor of PKA, 6-22 amide (Fig. 3F). Furthermore, MBP-gB-P2 was phosphorylated by PKA (Fig. 3H, lane 1), while MBP-gB-P2-T887A was not (Fig. 3H, lane 2). The presence of each MBP fusion protein and the radiolabeled MBP-gB-P2 band was verified by CBB staining (Fig. 3A, C, E, and G). These results indicated that PKA phosphorylated Thr-887 of gB *in vitro*.

**Us3-dependent phosphorylation of gB Thr-887 in infected cells.** To investigate whether gB Thr-887 was phosphorylated in infected cells, we constructed recombinant viruses YK551, in which gB Thr-887 was replaced with alanine, and YK553, in which the mutation was repaired (Fig. 1). The genotypes of YK551 and YK553 were confirmed by PCR analyses and sequencing (data not shown). Vero cells were infected with wild-type HSV-1(F), YK551 (gB-T887A), and YK553 (gB-TA-repair) at a multiplicity of infection (MOI) of 3, harvested at 18 h postinfection, solubilized and immunoprecipitated with anti-gB antibody, and analyzed by immunoblotting with anti-phospho-PKA substrate antibody or anti-gB antibody as described previously (18). As shown in Fig. 4, anti-phospho-PKA substrate antibody reacted with wild-type gB purified from HSV-1(F)-infected Vero cells by immunoprecipitation (Fig. 4A, lane 6, and C), while there was little reaction with gB-T887A purified from YK551-infected Vero cells (Fig. 4A, lane 7, and C). The wild-type phenotype was restored in cells infected with recombinant virus YK553, in which the T887A mutation in gB was repaired (Fig. 4A, lane 8, and C). To confirm that the wild-type gB detected by the anti-phospho-PKA substrate antibody was due to phosphorylation, wild-type gB purified by immunoprecipitation was treated with  $\lambda$ -PPase. As shown in Fig. 4E, the reactivity of wild-type gB with anti-phospho-PKA substrate antibody was eliminated by phosphatase treatment, confirming that the anti-phospho-PKA sub-

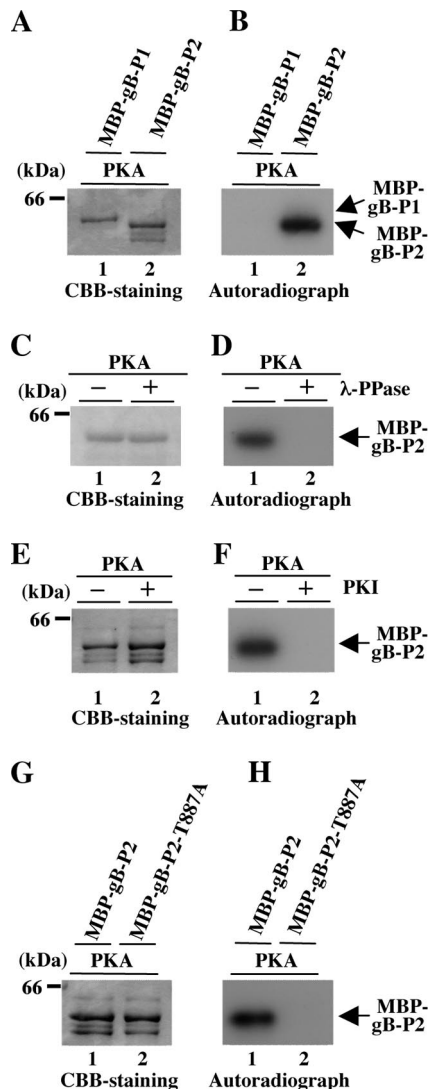


FIG. 3. (A) Purified MBP-gB-P1 (lane 1) and MBP-gB-P2 (lane 2) incubated in kinase buffer containing [ $\gamma$ - $^{32}$ P]ATP and purified PKA (lanes 1 and 2), separated on a denaturing gel, and stained with CBB. A molecular mass marker (in kilodaltons) is shown on the left. (B) Autoradiograph of the gel in panel A. (C) Purified MBP-gB-P2 incubated in kinase buffer containing [ $\gamma$ - $^{32}$ P]ATP and purified PKA and then either mock treated (lane 1) or treated with  $\lambda$ -PPase (lane 2), separated on a denaturing gel, and stained with CBB. A molecular mass marker (in kilodaltons) is shown on the left. (D) Autoradiograph of the gel in panel C. (E) Purified MBP-gB-P2 incubated in kinase buffer containing [ $\gamma$ - $^{32}$ P]ATP and purified PKA in the absence (lane 1) or in the presence of the PKA inhibitor (PKI) (lane 2), separated on a denaturing gel, and stained with CBB. A molecular mass marker (in kilodaltons) is shown on the left. (F) Autoradiograph of the gel in panel E. (G) Purified MBP-gB-P2 (lane 1) and MBP-gB-P2-T887A (lane 2) incubated in kinase buffer containing [ $\gamma$ - $^{32}$ P]ATP and purified PKA (lanes 1 and 2), separated on a denaturing gel, and stained with CBB. A molecular mass marker (in kilodaltons) is shown on the left. (H) Autoradiograph of the gel in panel G.

strate antibody had reacted with phosphorylated wild-type gB. These results indicated that the anti-phospho-PKA substrate antibody specifically recognized phosphorylated Thr-887 in gB and that gB Thr-887 was phosphorylated in infected cells.

We next examined whether the phosphorylation of gB Thr-

887 is dependent on Us3 kinase activity in infected cells. Therefore, Vero cells were infected at an MOI of 3 with wild-type HSV-1(F); YK511, which encodes the kinase-inactive Us3 mutant; Us3K220M, in which methionine replaces the lysine codon at position 220 (Lys-220) in Us3; or YK513, in which the methionine replacement of Lys-220 in Us3 of YK511 had been repaired (18). Cells were harvested at 18 h postinfection, solubilized and immunoprecipitated with anti-gB antibody, and analyzed by immunoblotting with anti-phospho-PKA substrate antibody or anti-gB antibody. As shown in Fig. 4B, the phosphorylation of gB Thr-887 was significantly impaired in YK511 (Us3K220M)-infected cells compared to that of gB in wild-type virus-infected cells (Fig. 4B, lanes 6 and 7, and D). The wild-type phenotype was restored in cells infected with recombinant virus YK513, in which the K220M mutation in Us3 was repaired (Fig. 4B, lane 8, and D). These results indicated that Us3 protein kinase mediated the phosphorylation of gB Thr-887 in infected cells. We noted that gB Thr-887 was slightly phosphorylated in the absence of Us3 kinase activity in infected cells (Fig. 4B, lane 7, and D), indicating that a protein kinase(s) other than Us3, probably a cellular protein kinase(s), mediates the phosphorylation of gB Thr-887 in infected cells.

**Phosphorylation of gB Thr-887 and cell surface expression of gB.** Most envelope glycoproteins, such as gB and gD, are known to be expressed on the surface of infected cells (7). To examine the role of gB Thr-887 phosphorylation on the cell surface expression of gB in infected cells, Vero cells were infected with wild-type HSV-1(F), YK551 (gB-T887A), or YK553 (gB-TA-repair) at an MOI of 3 and harvested at 6 h postinfection. The expression of gB on the cell surface or the total accumulation of gB in infected cells was analyzed by flow cytometry. As shown in Fig. 5A, graph a, and B, the cell surface expression of mutant gB-T887A in Vero cells infected with YK551 (gB-T887A) was upregulated compared to that of wild-type gB in wild-type HSV-1(F)-infected cells. The wild-type phenotype was restored in Vero cells infected with recombinant virus YK553, in which the gB T887A mutation was repaired (Fig. 5A, graph b, and B). The total accumulation of gB-T887A mutant protein in Vero cells infected with YK551 (gB-T887A) was similar to that of wild-type gB protein in Vero cells infected with wild-type HSV-1(F) or the repaired virus YK553 (Fig. 5B). In contrast, the cell surface expression of gD in Vero cells infected with YK551 (gB-T887A) was similar to that of Vero cells infected with wild-type HSV-1(F) (Fig. 5A, graph c). Similar results were obtained at 18 h postinfection with Vero cells infected with each of the viruses (data not shown). Furthermore, the upregulation of the cell surface expression of the gB-T887A mutant also was observed with HEL cells (data not shown). Taken together with the observation described above that gB Thr-887 was a physiological Us3 phosphorylation site, these results suggested that the Us3 phosphorylation of gB Thr-887 caused the downregulation of gB expression on the surface of infected cells.

To confirm this hypothesis, two additional sets of experiments were performed. In the first set of experiments, we examined the effect of the gB-T887D mutation on gB cell surface expression or gB total accumulation in infected cells. It is known that the replacement of the target phosphorylation site with an acidic amino acid, such as glutamic acid or aspartic acid, sometimes mimics the negative charges produced by

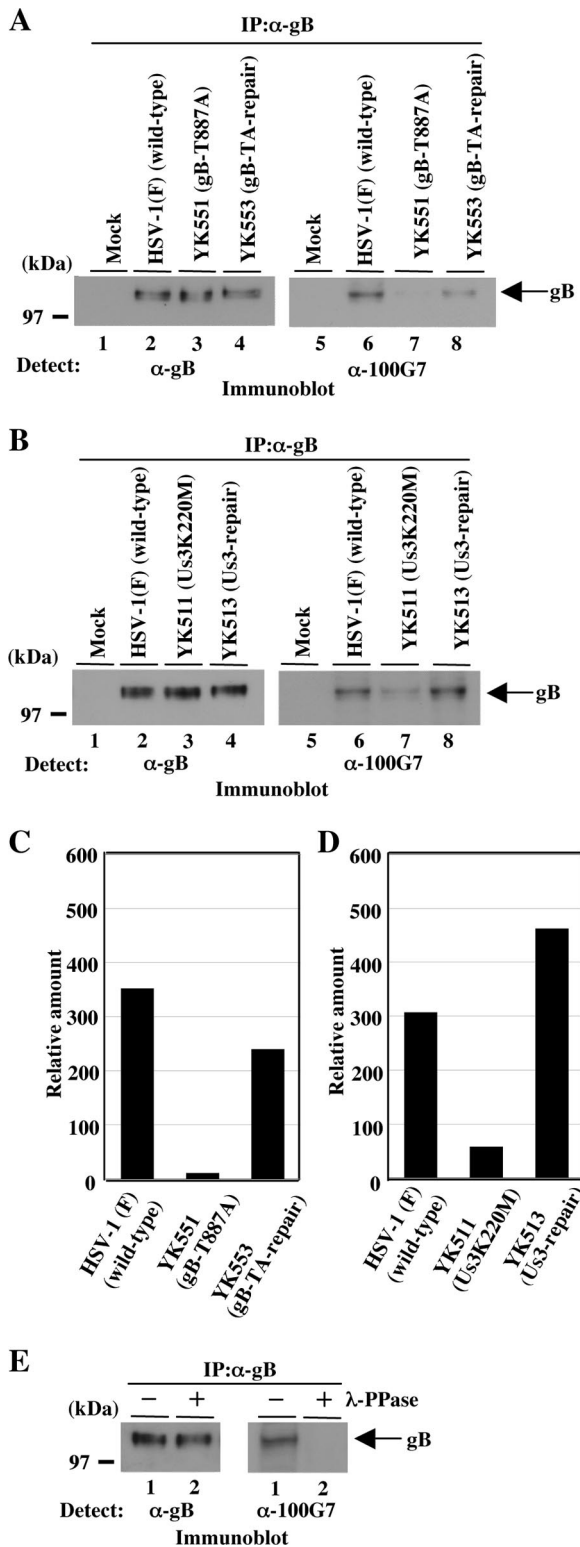


FIG. 4. (A) Immunoblots of electrophoretically separated gB immunoprecipitates (IP) from Vero cells mock infected (lanes 1 and 5) or infected with wild-type HSV-1(F) (lanes 2 and 6), YK551 (gB-T887A) (lanes 3 and 7), or YK553 (gB-TA-repair) (lanes 4 and 8) at an MOI of 3. The infected Vero cells were harvested 18 h postinfection and immunoprecipitated with anti-gB antibody (α-gB). The immunoprecipitates were separated on a denaturing gel, transferred to a polyvinylidene difluoride membrane, and analyzed by immunoblotting with anti-gB

phosphorylation (10, 61). Therefore, we generated two additional gB mutant viruses, YK555 (encoding the gB-T887D mutant) and YK557 (encoding its repaired codon, gB-TD-repair). The YK555 and YK557 genotypes were confirmed by PCR analyses and sequencing (data not shown). The expression of the predicted proteins was confirmed by infecting Vero cells with each of the recombinant viruses and assaying infected cells for the appropriate proteins by immunoblotting (Fig. 6, lanes 6 and 7). The results also indicated that the gB T887D mutation had no effect on the total accumulation of gB protein detected by immunoblotting in infected cells. As shown in Fig. 5A, graphs d and e, and B, the level of cell surface expression of gB-T887D or that of the total accumulation of gB-T887D in Vero cells infected with YK555 (gB-T887D) was almost identical to that of wild-type gB in cells infected with HSV-1(F) or YK557 (gB-TD-repair). Furthermore, the gB T887D mutation had no effect on the cell surface expression of gD in infected cells (Fig. 5A, graph f). Similar results were obtained at 18 h postinfection with Vero cells infected with each of the viruses as well as with HEL cells (data not shown).

In the second set of experiments, we tested whether the Us3 kinase activity controls the expression of gB on the cell surface of infected Vero cells. As described above (Fig. 4B), we showed that the phosphorylation of gB Thr-887 was dependent on Us3 kinase activity in infected cells. Therefore, if the cell surface expression of gB proteins is downregulated by the Us3 phosphorylation of gB Thr-887 in infected cells, it might be upregulated in the absence of Us3 kinase activity, as observed with the gB-T887A mutant in cells infected with YK551 (gB-T887A). As expected, the expression of gB on the surface of Vero cells infected with YK511 (Us3K220M) apparently was upregulated compared to that of wild-type HSV-1(F)-infected cells (Fig. 5A, graph g, and B). The wild-type phenotype was restored in Vero cells infected with recombinant virus YK513, in which the K220M mutation in Us3 was repaired (Fig. 5A, graph h, and B). The total accumulation of Us3K220A mutant protein in Vero cells infected with YK511 (Us3K220M) was similar to that of wild-type gB protein in Vero cells infected with wild-type HSV-1(F) or the repaired virus YK513 (Fig.

antibody (left) or anti-phospho-PKA substrate antibody (right). A molecular mass marker (in kilodaltons) is shown on the left. (B) Immunoblots of electrophoretically separated gB immunoprecipitates from Vero cells mock infected (lanes 1 and 5) or infected with wild-type HSV-1(F) (lanes 2 and 6), YK511 (Us3K220M) (lanes 3 and 7), or YK513 (Us3-repair) (lanes 4 and 8) at an MOI of 3. The infected Vero cells were harvested 18 h postinfection and immunoprecipitated with the anti-gB antibody. The immunoprecipitates were separated on a denaturing gel, transferred to a polyvinylidene difluoride membrane, and analyzed by immunoblotting with anti-gB antibody (left) or anti-phospho-PKA substrate antibody (right). A molecular mass marker (in kilodaltons) is shown on the left. (C and D) Quantitation of the relative amounts of phosphorylated gB proteins detected with anti-phospho-PKA substrate antibody, normalized to that of total gB proteins detected with anti-gB antibody shown in panels A and B, respectively. (E) Immunoprecipitates prepared as described for panel A, either mock treated (lanes 1) or treated with λ-PPase (lanes 2), separated on a denaturing gel, transferred to a polyvinylidene difluoride membrane, and analyzed by immunoblotting with anti-gB antibody (left) or anti-phospho-PKA substrate antibody (right). A molecular mass marker (in kilodaltons) is shown on the left.



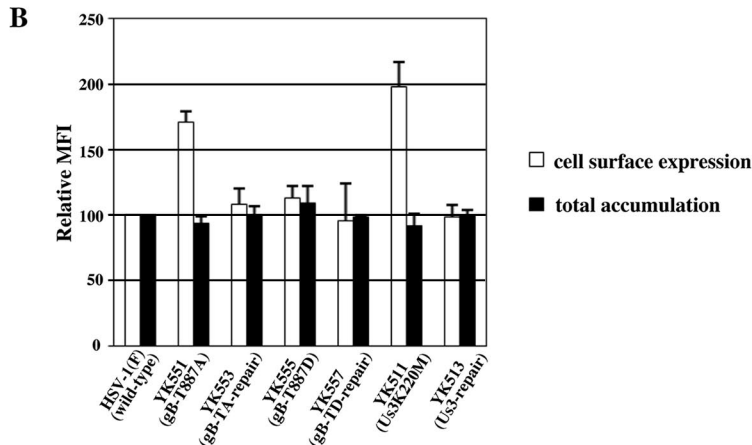
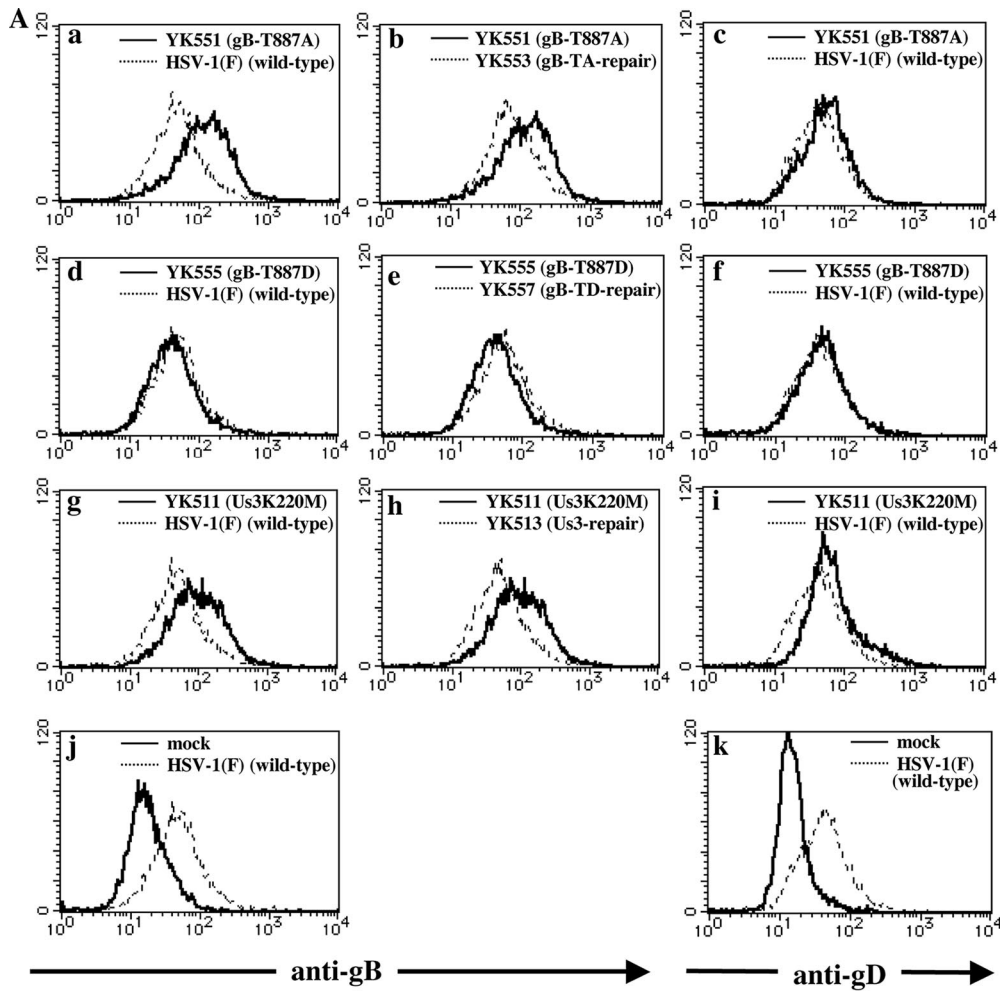


FIG. 5. (A) Detection of gB molecules on the surface of infected cells by flow cytometry using anti-gB (a, b, d, e, g, h and j) and anti-gD antibody (c, f, i, and k). Vero cells were mock infected or infected with wild-type HSV-1(F), YK551 (gB-T887A), YK553 (gB-TA-repair), YK555 (gB-T887D), YK557 (gB-TD-repair), YK511 (Us3K220M), or YK513 (Us3-repair) at an MOI of 3. At 6 h postinfection, infected cells were incubated with anti-gB or anti-gD antibody and then analyzed by flow cytometry. Each panel shows the cell surface expression of gB or gD in cells infected with one of the two indicated viruses. (B) Quantitation of the cell surface expression of gB (white bars) and the total accumulation of gB (black bars) in infected cells. Vero cells were infected with each of the indicated viruses and analyzed by flow cytometry as described for panel A. The mean fluorescent intensity (MFI) for mock-infected Vero cells was subtracted from the MFI for Vero cells infected with each of the viruses, and the relative MFI are shown as values relative to those of wild-type HSV-1(F). The results represent the averages from three independent experiments, and the standard deviations are presented.

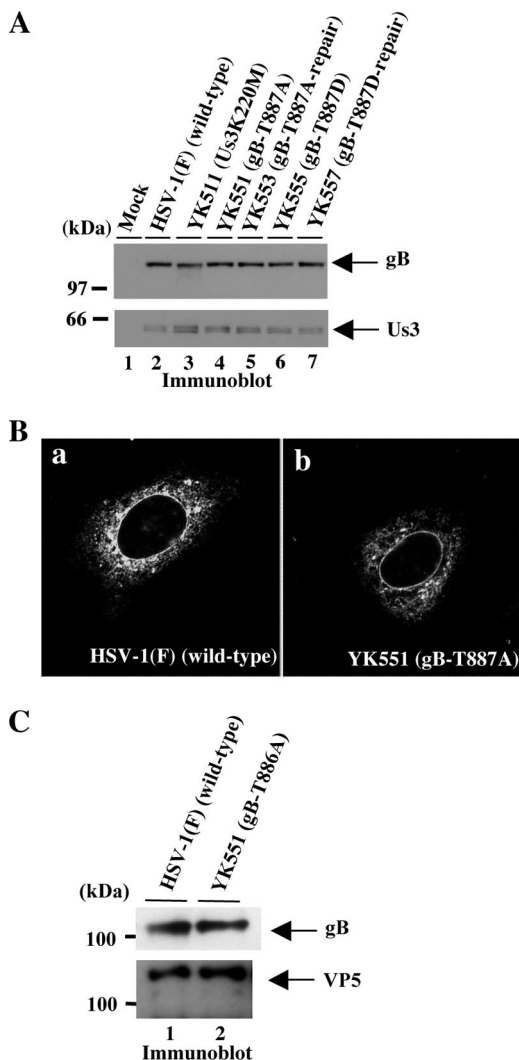


FIG. 6. (A) Immunoblots of electrophoretically separated lysates of Vero cells mock infected (lane 1) or infected with wild-type HSV-1(F) (lane 2), YK511 (Us3K220M) (lane 3), YK551 (gB-T887A) (lane 4), YK553 (gB-TA-repair) (lane 5), YK555 (gB-T887D) (lane 6), or YK557 (gB-TD-repair) (lane 7) at an MOI of 3. Infected Vero cells were harvested 18 h postinfection and analyzed by immunoblotting with antibody to gB (upper) or Us3 (lower). Molecular masses (in kilodaltons) are shown on the left. (B) Digital confocal images showing the localization of gB. Vero cells were infected with HSV-1(F) (a) or YK551 (b) at an MOI of 10 for 12 h and then fixed, permeabilized, stained with antibody to gB, and examined by confocal microscopy. (C) Immunoblots of electrophoretically separated virions of wild-type HSV-1(F) (lane 1) or YK551 (gB-T887A) purified by sucrose gradient centrifugation and reacted with antibody to gB (upper) or VP5 (lower). Molecular masses (in kilodaltons) are shown on the left.

5B). In contrast, the upregulation of the cell surface expression of gD was barely detected in Vero cells infected with YK511 (Us3K220M) (Fig. 5A, graph i). Similar results were obtained at 18 h postinfection for Vero cells infected with each of the viruses (data not shown). Furthermore, the upregulation of the cell surface expression of gB also was observed with HEL cells infected with YK511 (Us3K220M) (data not shown).

Taken together, these observations support the hypothesis

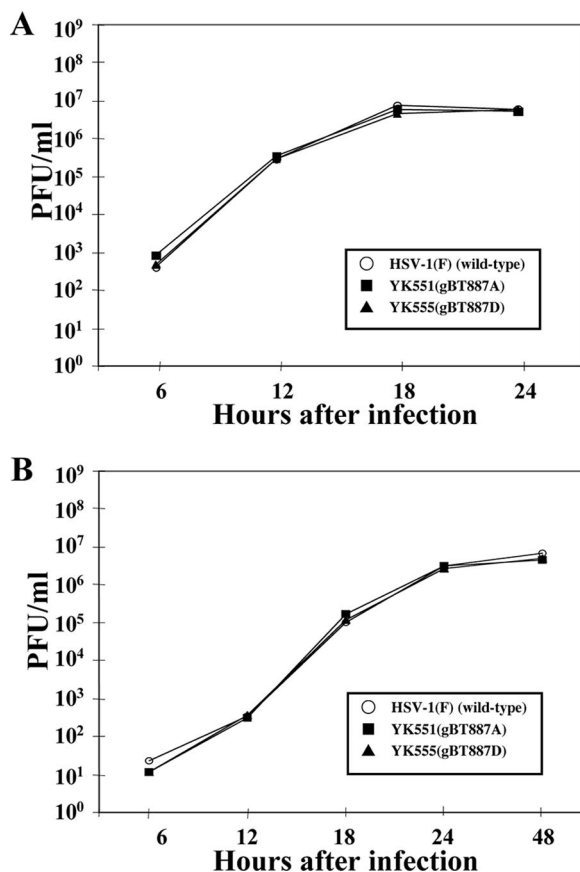


FIG. 7. Growth curves of wild-type and recombinant viruses. Vero cells were infected with wild-type HSV-1(F) (open circles), YK551 (gB-T887A) (filled squares), or YK555 (gB-T887D) (filled triangles) at an MOI of 3 (A) or 0.01 (B). For each experiment, total virus from infected cells and cell culture supernatants was harvested at the indicated times and assayed on Vero cells.

that the cell surface expression of gB was downregulated by the Us3 phosphorylation of gB Thr-887 in infected cells.

**Phosphorylation of gB Thr-887 and virus replication.** To investigate the role(s) of gB Thr-887 phosphorylation on viral replication in cell cultures, three sets of experiments were performed. In the first set of experiments, growth curves of YK551 (gB-T887A) and wild-type HSV-1(F) were analyzed by infecting Vero cells with each virus at an MOI of 3 or 0.01, harvesting total virus from the infected cells and cell culture supernatants at several times postinfection, and assaying each sample for PFU on Vero cells. As shown in Fig. 7, the growth curves of YK551 (gB-T887A) and wild-type HSV-1(F) on Vero cells at both MOIs were essentially identical. We also noted that plaques produced by both YK551 (gB-T887A) and wild-type HSV-1(F) were of similar size on Vero cells (data not shown). In the second set of experiments, Vero cells were infected with YK551 (gB-T887A) or HSV-1(F) at an MOI of 3 or 0.01, and secreted extracellular virus and cell-associated virus were harvested separately and assayed for PFU. These results showed that the growth curves of cell-associated and extracellular YK551 (gB-T887A) viruses were almost identical to those of wild-type HSV-1(F) (data not shown). In the third set of experiments, HEL or SK-N-SH cells were infected with



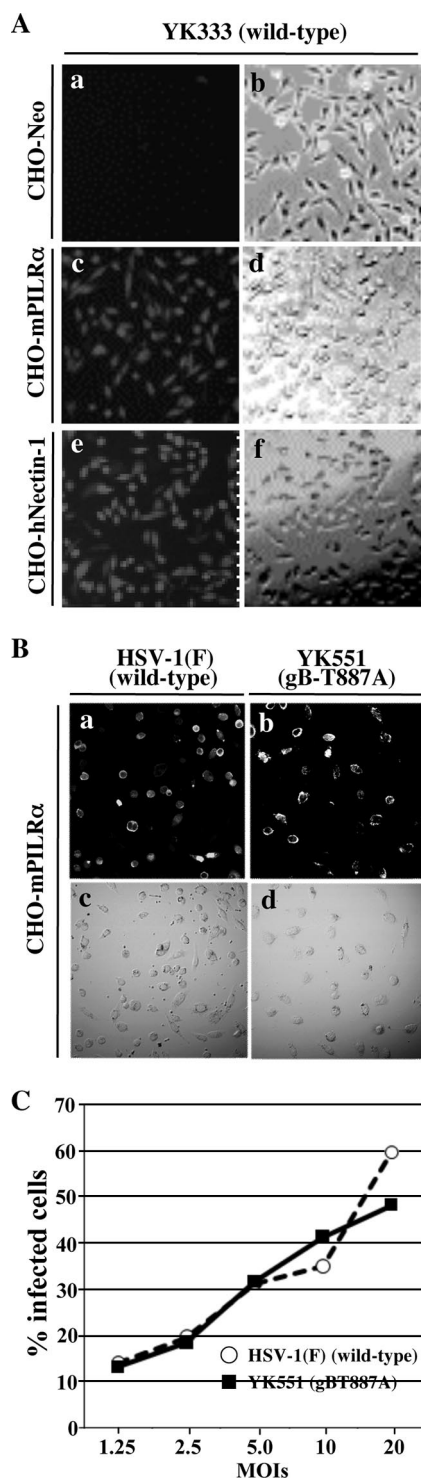


FIG. 8. (A) Digital fluorescent microscopic images showing infection of CHO-neo (a and b), CHO-mPILR $\alpha$  (c and d), or CHO-hnectin-1 cells (e and f) with YK333 at an MOI of 50. At 10 h postinfection, live infected cells were examined by fluorescence microscopy. Fluorescent (a, c, and e) and phase-contrast images (b, d, and f) of infected cells are shown. (B) Digital confocal images showing the infection of CHO-mPILR $\alpha$  cells with wild-type HSV-1(F) (a and c) or YK551 (gB-T887A) (b and d) at an MOI of 10. At 12 h postinfection, infected cells were fixed, permeabilized, stained with anti-ICP0 antibody, and then examined by confocal microscopy. Fluorescence (a and b) and differential interference contrast (c and d) images of infected cells are

YK551 (gB-T887A) or HSV-1(F) at an MOI of 3 or 0.01. For cells infected at an MOI of 3, extracellular and cell-associated viruses were harvested separately at 24 h postinfection, whereas for cells infected at an MOI of 0.01, extracellular and cell-associated viruses were harvested separately at 24 and 48 h postinfection. The results showed that the yields of extracellular and cell-associated viruses for infection with YK551 (gB-T887A) in HEL and SK-N-SH cells were almost identical to those for wild-type HSV-1(F) at MOIs of 3 and 0.01 (data not shown). These results indicated that gB with either Thr-887 or phosphorylated Thr-887 was not required for optimal virus replication in cell cultures.

To test whether the phosphorylation of gB Thr-887 regulated the total accumulation and intracellular localization of gB proteins in infected cells, Vero cells were infected with HSV-1(F) or YK551 and analyzed by immunoblotting and immunofluorescence with confocal microscopy. The results showed that the expression levels (Fig. 6A, lanes 2 and 4) and intracellular localization (Fig. 6B) of gB-T887A mutant protein in Vero cells infected with YK551 were similar to those of wild-type gB protein in Vero cells infected with wild-type HSV-1(F). These results indicated that gB with either Thr-887 or phosphorylated Thr-887 was not involved in the regulation of total gB accumulation, as determined by immunoblotting, and of intracellular gB localization, as determined by immunofluorescence in fixed cells. These results are consistent with those shown in Fig. 5B. We next compared the incorporation of gB-T887A mutant protein into YK551 virions to that of wild-type gB into wild-type virions by purifying virions and analyzing them by immunoblotting with anti-gB antibody. The results (Fig. 6C) showed that the amount of gB-T887A protein in YK551 virions was similar to that of wild-type gB in wild-type virions, indicating that gB with Thr-887 or phosphorylated Thr-887 does not regulate the efficiency of gB packaging into virions.

Finally, we analyzed the entry of YK551 and wild-type HSV-1(F) viruses into cells via the PILR $\alpha$  gB receptor (51). For this study, we generated PILR ligand-negative CHO-K1 cells stably expressing mouse PILR $\alpha$  to facilitate monitoring PILR $\alpha$ -dependent virus entry. In agreement with a previous report (51), the stable expression of PILR $\alpha$  on PILR ligand-negative CHO-K1 cells resulted in a significant increase in YK333 infection (Fig. 8A), as was observed with the stable expression of a gD receptor, nectin-1, on PILR ligand-negative CHO-K1 cells. As shown in Fig. 8B, the efficiency of the infection of the PILR $\alpha$ -expressing CHO-K1 cells with YK551 at an MOI of 10 and detected by ICP0 expression (58% of cells) was similar to that of wild-type HSV-1(F) (62% of cells). Similar results were obtained with infected cells at different MOIs (Fig. 8C). These results indicated that gB with Thr-887 or phosphorylated Thr-887 is not required for virus entry into cells via PILR $\alpha$ .

shown. (C) Proportion of CHO-mPILR $\alpha$  cells infected with wild-type YK304 (closed square) or YK551 (gB-T887A) (open circle) at the indicated MOIs. At 12 h postinfection, infected cells were fixed, permeabilized, stained with anti-ICP4 antibody, and then examined by flow cytometry.



887 also regulated the cell surface expression of gB. It is unknown at present how gB phosphorylation by Us3 controls the cell surface expression of gB. It may be that gB phosphorylation mediated by Us3 regulates one or more of the following steps: the direct sorting of newly synthesized gB to the cell surface, the internalization of gB by endocytosis, and the recycling of internalized gB to the cell surface. Since Thr-887 is very close to the YTQV motif (residues 889 to 892) (Fig. 9), a conformational change in gB mediated by the Us3 phosphorylation of gB Thr-887 might affect the recognition of the endocytosis motif by AP complexes. This interpretation might also argue for the possibility that the phenotype observed for recombinant virus with mutations in gB Thr-887 is due to the steric hindrance of gB caused by the amino acid replacements, rather than being due to the prevention and mimicry of gB Thr-887 phosphorylation, leading to an effect on the endocytosis motif; the cell surface expression of gB could be upregulated. However, this possibility is less likely, based on the observation that the effect of the K220M mutation in Us3, which greatly impaired the phosphorylation of gB Thr-887, on the cell surface expression of gB was identical to that of the gB T887A mutation, which prevented the phosphorylation of Thr-887. Furthermore, the effect of the gB-T887D mutation, which was predicted to mimic the phosphorylation of Thr-887, was different from that of T887A in gB, and the phenotype of the gB-T887D virus was identical to that of wild-type virus.

It has been reported that gB on the cell surface is a potent inducer of the immune response *in vivo* (4, 5, 49, 50), and it has been speculated that the downregulation of the cell surface expression of gB by endocytosis could involve immune evasion (7). In fact, the lysis of HSV-1-infected cells by natural killer cells correlates with the cell surface expression of gB (4). The Us3 phosphorylation of gB, which decreases the number of gB molecules on the cell surface exposed to the immune system, may make it difficult for infected cells to be recognized and attacked by the immune system *in vivo*. Therefore, it is of interest to examine whether YK551 (gB-T887A) infection is attenuated in animal models as it is in Us3 deletion mutant viruses (30), and these studies are in progress in this laboratory. Furthermore, our observations raise the interesting possibility that Us3 also downregulates other cell surface molecules in infected cells that might be involved in immune evasion. In agreement with this possibility, a Us3 homologue (ORF66) in varicella-zoster virus has been reported to mediate the downregulation of the cell surface expression of a class I major histocompatibility complex (11). Finally, we note that gB Thr-887 is conserved among HSV-1 strains but not among other alphaherpesvirus gB homologues. Even HSV-2 gB protein lacks a comparable threonine residue (Fig. 9). This suggests that the Us3 phosphorylation of gB Thr-887 and its relevance for the regulation of cell surface gB expression are specific to HSV-1. In agreement with this, we previously reported that a physiological autophosphorylation site in Us3 that regulates the proper localization of the viral kinase and the morphology of infected cells is not conserved among other alphaherpesviruses, including HSV-2 (18). These observations suggest that HSV-1 evolved unique strategies to modify the functions of gB and Us3 and, possibly, yet-to-be-reported viral proteins. These possibilities might be significant for under-

standing the pathological differences between HSV-1 and HSV-2.

#### ACKNOWLEDGMENTS

We thank Gregory A. Smith for *E. coli* GS1783, Nikolaus Osterrieder for *E. coli* GS1783 containing pYBac102, Toshio Kitamura for Plat-GP cells and pMxs-Neo, and Didier Trono for pMD-G. We thank David Johnson for helpful discussions. We are grateful to Shihoko Koyama for excellent technical assistance. We thank Masayuki Shimomima for technical assistance with fluorescence-activated cell sorting.

This study was supported in part by grants for scientific research and grants for scientific research in priority areas from the Ministry of Education, Culture, Science, Sports and Technology (MEXT) of Japan and a grant from the Takeda Science Foundation. A.K. and J.A. were supported by a research fellowship of the Japanese Society for the Promotion of Science (JSPS) for Young Scientists.

#### REFERENCES

1. **Beitia Ortiz de Zarate, I., L. Cantero-Aguilar, M. Longo, C. Berlioz-Torrent, and F. Rozenberg.** 2007. Contribution of endocytic motifs in the cytoplasmic tail of herpes simplex virus type 1 glycoprotein B to virus replication and cell-cell fusion. *J. Virol.* **81**:13889–13903.
2. **Bender, F. C., J. C. Whitbeck, H. Lou, G. H. Cohen, and R. J. Eisenberg.** 2005. Herpes simplex virus glycoprotein B binds to cell surfaces independently of heparan sulfate and blocks virus entry. *J. Virol.* **79**:11588–11597.
3. **Benetti, L., and B. Roizman.** 2004. Herpes simplex virus protein kinase US3 activates and functionally overlaps protein kinase A to block apoptosis. *Proc. Natl. Acad. Sci. USA* **101**:9411–9416.
4. **Bishop, G. A., J. C. Glorioso, and S. A. Schwartz.** 1983. Relationship between expression of herpes simplex virus glycoproteins and susceptibility of target cells to human natural killer activity. *J. Exp. Med.* **157**:1544–1561.
5. **Bishop, G. A., S. D. Marlin, S. A. Schwartz, and J. C. Glorioso.** 1984. Human natural killer cell recognition of herpes simplex virus type 1 glycoproteins: specificity analysis with the use of monoclonal antibodies and antigenic variants. *J. Immunol.* **133**:2206–2214.
6. **Bonifacino, J. S., and L. M. Traub.** 2003. Signals for sorting of transmembrane proteins to endosomes and lysosomes. *Annu. Rev. Biochem.* **72**:395–447.
7. **Brideau, A. D., L. W. Enquist, and R. S. Tirabassi.** 2000. The role of virion membrane protein endocytosis in the herpesvirus life cycle. *J. Clin. Virol.* **17**:69–82.
8. **Daikoku, T., Y. Yamashita, T. Tsurumi, K. Maeno, and Y. Nishiyama.** 1993. Purification and biochemical characterization of the protein kinase encoded by the US3 gene of herpes simplex virus type 2. *Virology* **197**:685–694.
9. **Edelman, A. M., D. K. Blumenthal, and E. G. Krebs.** 1987. Protein serine/threonine kinases. *Annu. Rev. Biochem.* **56**:567–613.
10. **Eisfeld, A. J., S. E. Turse, S. A. Jackson, E. C. Lerner, and P. R. Kinchington.** 2006. Phosphorylation of the varicella-zoster virus (VZV) major transcriptional regulatory protein IE62 by the VZV open reading frame 66 protein kinase. *J. Virol.* **80**:1710–1723.
11. **Eisfeld, A. J., M. B. Yee, A. Erazo, A. Abendroth, and P. R. Kinchington.** 2007. Downregulation of class I major histocompatibility complex surface expression by varicella-zoster virus involves open reading frame 66 protein kinase-dependent and -independent mechanisms. *J. Virol.* **81**:9034–9049.
12. **Ejercito, P. M., E. D. Kieff, and B. Roizman.** 1968. Characterization of herpes simplex virus strains differing in their effects on social behaviour of infected cells. *J. Gen. Virol.* **2**:357–364.
13. **Farnsworth, A., T. W. Wisner, M. Webb, R. Roller, G. Cohen, R. Eisenberg, and D. C. Johnson.** 2007. Herpes simplex virus glycoproteins gB and gH function in fusion between the virion envelope and the outer nuclear membrane. *Proc. Natl. Acad. Sci. USA* **104**:10187–10192.
14. **Favoreel, H. W., G. Van Minnebruggen, H. J. Nauwynck, L. W. Enquist, and M. B. Pensaert.** 2002. A tyrosine-based motif in the cytoplasmic tail of pseudorabies virus glycoprotein B is important for both antibody-induced internalization of viral glycoproteins and efficient cell-to-cell spread. *J. Virol.* **76**:6845–6851.
15. **Frame, M. C., F. C. Purves, D. J. McGeoch, H. S. Marsden, and D. P. Leader.** 1987. Identification of the herpes simplex virus protein kinase as the product of viral gene US3. *J. Gen. Virol.* **68**:2699–2704.
16. **Geraghty, R. J., C. Krummenacher, G. H. Cohen, R. J. Eisenberg, and P. G. Spear.** 1998. Entry of alphaherpesviruses mediated by poliovirus receptor-related protein 1 and poliovirus receptor. *Science* **280**:1618–1620.
17. **Jarosinski, K. W., N. G. Margulis, J. P. Kamil, S. J. Spatz, V. K. Nair, and N. Osterrieder.** 2007. Horizontal transmission of Marek's disease virus requires US2, the UL13 protein kinase, and gC. *J. Virol.* **81**:10575–10587.
18. **Kato, A., M. Tanaka, M. Yamamoto, R. Asai, T. Sata, Y. Nishiyama, and Y. Kawaguchi.** 2008. Identification of a physiological phosphorylation site of



- the herpes simplex virus 1-encoded protein kinase Us3 which regulates its optimal catalytic activity in vitro and influences its function in infected cells. *J. Virol.* **82**:6172–6189.
19. **Kato, A., M. Yamamoto, T. Ohno, H. Kodaira, Y. Nishiyama, and Y. Kawaguchi.** 2005. Identification of proteins phosphorylated directly by the Us3 protein kinase encoded by herpes simplex virus 1. *J. Virol.* **79**:9325–9331.
  20. **Kato, A., M. Yamamoto, T. Ohno, M. Tanaka, T. Sata, Y. Nishiyama, and Y. Kawaguchi.** 2006. Herpes simplex virus 1-encoded protein kinase UL13 phosphorylates viral Us3 protein kinase and regulates nuclear localization of viral envelopment factors UL34 and UL31. *J. Virol.* **80**:1476–1486.
  21. **Kawaguchi, Y., and K. Kato.** 2003. Protein kinases conserved in herpesviruses potentially share a function mimicking the cellular protein kinase cdc2. *Rev. Med. Virol.* **13**:331–340.
  22. **Kawaguchi, Y., K. Kato, M. Tanaka, M. Kanamori, Y. Nishiyama, and Y. Yamanashi.** 2003. Conserved protein kinases encoded by herpesviruses and cellular protein kinase cdc2 target the same phosphorylation site in eukaryotic elongation factor 1delta. *J. Virol.* **77**:2359–2368.
  23. **Kawaguchi, Y., C. Van Sant, and B. Roizman.** 1998. Eukaryotic elongation factor 1δ is hyperphosphorylated by the protein kinase encoded by the UL13 gene of herpes simplex virus 1. *J. Virol.* **72**:1731–1736.
  24. **Kawaguchi, Y., C. Van Sant, and B. Roizman.** 1997. Herpes simplex virus 1α regulatory protein ICP0 interacts with and stabilizes the cell cycle regulator cyclin D3. *J. Virol.* **71**:7328–7336.
  25. **Leader, D. P.** 1993. Viral protein kinases and protein phosphatases. *Pharmacol. Ther.* **59**:343–389.
  26. **Leader, D. P., A. D. Deana, F. Marchiori, F. C. Purves, and L. A. Pinna.** 1991. Further definition of the substrate specificity of the alpha-herpesvirus protein kinase and comparison with protein kinases A and C. *Biochim. Biophys. Acta* **1091**:426–431.
  27. **Leopardi, R., C. Van Sant, and B. Roizman.** 1997. The herpes simplex virus 1 protein kinase US3 is required for protection from apoptosis induced by the virus. *Proc. Natl. Acad. Sci. USA* **94**:7891–7896.
  28. **Manning, G., D. B. Whyte, R. Martinez, T. Hunter, and S. Sudarsanam.** 2002. The protein kinase complement of the human genome. *Science* **298**:1912–1934.
  29. **McGeoch, D. J., and A. J. Davison.** 1986. Alphaherpesviruses possess a gene homologous to the protein kinase gene family of eukaryotes and retroviruses. *Nucleic Acids Res.* **14**:1765–1777.
  30. **Meignier, B., R. Longnecker, P. Mavromara-Nazos, A. E. Sears, and B. Roizman.** 1988. Virulence of and establishment of latency by genetically engineered deletion mutants of herpes simplex virus 1. *Virology* **162**:251–254.
  31. **Montgomery, R. I., M. S. Warner, B. J. Lum, and P. G. Spear.** 1996. Herpes simplex virus-1 entry into cells mediated by a novel member of the TNF/NGF receptor family. *Cell* **87**:427–436.
  32. **Morita, S., T. Kojima, and T. Kitamura.** 2000. Plat-E: an efficient and stable system for transient packaging of retroviruses. *Gene Ther.* **7**:1063–1066.
  33. **Mou, F., T. Forest, and J. D. Baines.** 2007. US3 of herpes simplex virus type 1 encodes a promiscuous protein kinase that phosphorylates and alters localization of lamin A/C in infected cells. *J. Virol.* **81**:6459–6470.
  34. **Munger, J., A. V. Chee, and B. Roizman.** 2001. The US<sub>3</sub> protein kinase blocks apoptosis induced by the d120 mutant of herpes simplex virus 1 at a premitochondrial stage. *J. Virol.* **75**:5491–5497.
  35. **Munger, J., and B. Roizman.** 2001. The US3 protein kinase of herpes simplex virus 1 mediates the posttranslational modification of BAD and prevents BAD-induced programmed cell death in the absence of other viral proteins. *Proc. Natl. Acad. Sci. USA* **98**:10410–10415.
  36. **Murata, T., F. Goshima, Y. Nishizawa, T. Daikoku, H. Takakuwa, K. Ohtsuka, T. Yoshikawa, and Y. Nishiyama.** 2002. Phosphorylation of cytokeratin 17 by herpes simplex virus type 2 US3 protein kinase. *Microbiol. Immunol.* **46**:707–719.
  37. **Ogg, P. D., P. J. McDonell, B. J. Ryckman, C. M. Knudson, and R. J. Roller.** 2004. The HSV-1 Us3 protein kinase is sufficient to block apoptosis induced by overexpression of a variety of Bcl-2 family members. *Virology* **319**:212–224.
  38. **Pellett, P. E., K. G. Kousoulas, L. Pereira, and B. Roizman.** 1985. Anatomy of the herpes simplex virus 1 strain F glycoprotein B gene: primary sequence and predicted protein structure of the wild type and of monoclonal antibody-resistant mutants. *J. Virol.* **53**:243–253.
  39. **Pellett, P. E., and B. Roizman.** 2007. The family *Herpesviridae*: a brief introduction, p. 2479–2499. *In* D. M. Knipe, P. M. Howley, D. E. Griffin, R. A. Lamb, M. A. Martin, B. Roizman, and S. E. Straus (ed.), *Fields virology*, 5th ed. Lippincott Williams & Wilkins, Philadelphia, PA.
  40. **Purves, F. C., A. D. Deana, F. Marchiori, D. P. Leader, and L. A. Pinna.** 1986. The substrate specificity of the protein kinase induced in cells infected with herpesviruses: studies with synthetic substrates [corrected] indicate structural requirements distinct from other protein kinases. *Biochim. Biophys. Acta* **889**:208–215.
  41. **Purves, F. C., R. M. Longnecker, D. P. Leader, and B. Roizman.** 1987. Herpes simplex virus 1 protein kinase is encoded by open reading frame US3 which is not essential for virus growth in cell culture. *J. Virol.* **61**:2896–2901.
  42. **Purves, F. C., W. O. Ogle, and B. Roizman.** 1993. Processing of the herpes simplex virus regulatory protein alpha 22 mediated by the UL13 protein kinase determines the accumulation of a subset of alpha and gamma mRNAs and proteins in infected cells. *Proc. Natl. Acad. Sci. USA* **90**:6701–6705.
  43. **Purves, F. C., D. Spector, and B. Roizman.** 1991. The herpes simplex virus 1 protein kinase encoded by the US3 gene mediates posttranslational modification of the phosphoprotein encoded by the UL34 gene. *J. Virol.* **65**:5757–5764.
  44. **Reynolds, A. E., B. J. Ryckman, J. D. Baines, Y. Zhou, L. Liang, and R. J. Roller.** 2001. U<sub>L</sub>31 and U<sub>L</sub>34 proteins of herpes simplex virus type 1 form a complex that accumulates at the nuclear rim and is required for envelopment of nucleocapsids. *J. Virol.* **75**:8803–8817.
  45. **Reynolds, A. E., E. G. Wills, R. J. Roller, B. J. Ryckman, and J. D. Baines.** 2002. Ultrastructural localization of the herpes simplex virus type 1 UL31, UL34, and US3 proteins suggests specific roles in primary envelopment and egress of nucleocapsids. *J. Virol.* **76**:8939–8952.
  46. **Roizman, B., D. M. Knipe, and R. J. Whitley.** 2007. Herpes simplex viruses, p. 2501–2602. *In* D. M. Knipe, P. M. Howley, D. E. Griffin, R. A. Lamb, M. A. Martin, B. Roizman, and S. E. Straus (ed.), *Fields virology*, 5th ed. Lippincott Williams & Wilkins, Philadelphia, PA.
  47. **Roller, R. J., Y. Zhou, R. Schnetzer, J. Ferguson, and D. DeSalvo.** 2000. Herpes simplex virus type 1 U<sub>L</sub>34 gene product is required for viral envelopment. *J. Virol.* **74**:117–129.
  48. **Ryckman, B. J., and R. J. Roller.** 2004. Herpes simplex virus type 1 primary envelopment: UL34 protein modification and the US3-UL34 catalytic relationship. *J. Virol.* **78**:399–412.
  49. **Sanchez-Pescador, L., P. Paz, D. Navarro, L. Pereira, and S. Kohl.** 1992. Epitopes of herpes simplex virus type 1 glycoprotein B that bind type-common neutralizing antibodies elicit type-specific antibody-dependent cellular cytotoxicity. *J. Infect. Dis.* **166**:623–627.
  50. **Sanchez-Pescador, L., L. Pereira, E. D. Charlebois, and S. Kohl.** 1993. Antibodies to epitopes of herpes simplex virus type 1 glycoprotein B (gB) in human sera: analysis of functional gB epitopes defined by inhibition of murine monoclonal antibodies. *J. Infect. Dis.* **168**:844–853.
  51. **Satoh, T., J. Arii, T. Suenaga, J. Wang, A. Kogure, J. Uehori, N. Arase, I. Shiratori, S. Tanaka, Y. Kawaguchi, P. G. Spear, L. L. Lanier, and H. Arase.** 2008. PILRα is a herpes simplex virus-1 entry coreceptor that associates with glycoprotein B. *Cell* **132**:935–944.
  52. **Shukla, D., J. Liu, P. Blaiklock, N. W. Shworak, X. Bai, J. D. Esko, G. H. Cohen, R. J. Eisenberg, R. D. Rosenberg, and P. G. Spear.** 1999. A novel role for 3-O-sulfated heparan sulfate in herpes simplex virus 1 entry. *Cell* **99**:13–22.
  53. **Shukla, D., and P. G. Spear.** 2001. Herpesviruses and heparan sulfate: an intimate relationship in aid of viral entry. *J. Clin. Investig.* **108**:503–510.
  54. **Spear, P. G.** 2004. Herpes simplex virus: receptors and ligands for cell entry. *Cell Microbiol.* **6**:401–410.
  55. **Tanaka, M., H. Kagawa, Y. Yamanashi, T. Sata, and Y. Kawaguchi.** 2003. Construction of an excisable bacterial artificial chromosome containing a full-length infectious clone of herpes simplex virus type 1: viruses reconstituted from the clone exhibit wild-type properties in vitro and in vivo. *J. Virol.* **77**:1382–1391.
  56. **Tanaka, M., H. Kodaira, Y. Nishiyama, T. Sata, and Y. Kawaguchi.** 2004. Construction of recombinant herpes simplex virus type I expressing green fluorescent protein without loss of any viral genes. *Microbes Infect.* **6**:485–493.
  57. **Tanaka, M., Y. Nishiyama, T. Sata, and Y. Kawaguchi.** 2005. The role of protein kinase activity expressed by the UL13 gene of herpes simplex virus 1: the activity is not essential for optimal expression of UL41 and ICP0. *Virology* **341**:301–312.
  58. **Wang, J., I. Shiratori, T. Satoh, L. L. Lanier, and H. Arase.** 2008. An essential role of sialylated O-linked sugar chains in the recognition of mouse CD99 by paired Ig-like type 2 receptor (PILR). *J. Immunol.* **180**:1686–1693.
  59. **Warner, M. S., R. J. Geraghty, W. M. Martinez, R. I. Montgomery, J. C. Whitbeck, R. Xu, R. J. Eisenberg, G. H. Cohen, and P. G. Spear.** 1998. A cell surface protein with herpesvirus entry activity (HvE) confers susceptibility to infection by mutants of herpes simplex virus type 1, herpes simplex virus type 2, and pseudorabies virus. *Virology* **246**:179–189.
  60. **Wisner, T. W., and D. C. Johnson.** 2004. Redistribution of cellular and herpes simplex virus proteins from the *trans*-Golgi network to cell junctions without enveloped capsids. *J. Virol.* **78**:11519–11535.
  61. **Yokoyama, A., M. Tanaka, G. Matsuda, K. Kato, M. Kanamori, H. Kawasaki, H. Hirano, I. Kitabayashi, M. Ohki, K. Hirai, and Y. Kawaguchi.** 2001. Identification of major phosphorylation sites of Epstein-Barr virus nuclear antigen leader protein (EBNA-LP): ability of EBNA-LP to induce latent membrane protein 1 cooperatively with EBNA-2 is regulated by phosphorylation. *J. Virol.* **75**:5119–5128.
  62. **Zufferey, R., D. Nagy, R. J. Mandel, L. Naldini, and D. Trono.** 1997. Multiply attenuated lentiviral vector achieves efficient gene delivery in vivo. *Nat. Biotechnol.* **15**:871–875.